

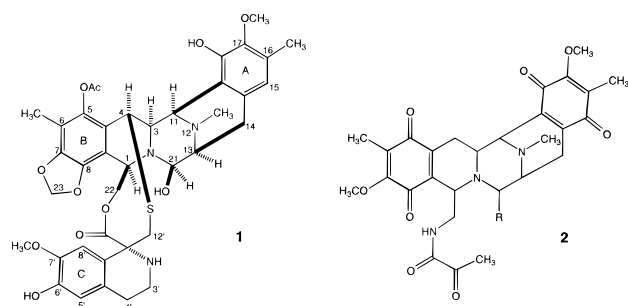
NMR-Based Model of an Ecteinascidin 743–DNA Adduct

Bob M. Moore, II, Frederick C. Seaman, and Laurence H. Hurley*

Drug Dynamics Institute, College of Pharmacy
The University of Texas at Austin, Austin, Texas 78712-1074

Received February 11, 1997

The ecteinascidins¹ (Ets) are extremely potent antitumor agents isolated from extracts of the marine tunicate *Ecteinascidia turbinata* that exhibit promising efficacy in several human xenograft models in mice.^{2,3} The structural novelty prompted researchers to isolate new ecteinascidin (Et) analogs,² determine the structure⁴ and absolute configuration of several Ets,² and complete the total synthesis of Et 743 (**1**).⁵ The first Et to



advance to clinical trials is **1**;² however, the mechanism of antitumor activity remains unclear. Bioassays using purified Ets demonstrated inhibitory activity toward DNA and RNA polymerases.² Sequence-selective high-affinity binding of **1** to duplex DNA⁶ suggests a mechanism of action involving DNA interactions. Additionally, the reactive carbinolamine of **1** is analogous to that found in known guanine N2 (GN2) DNA alkylating agents.⁷ The DNA-reactive saframycins (**2**) are structurally similar to the A and B units of **1**, and on the basis of this similarity, theoretical models of **1** bound to DNA have been proposed.⁴

Et 743 is reported to react with 5'-GGG, 5'-GGC, and 5'-AGC DNA sequences;⁶ therefore, in order to assess alkylation selectivity, **1** was reacted with an oligonucleotide containing 5'-GGC (strand 1) and 5'-AGC (strand 2) alkylation sites. A mixed oligonucleotide–drug adduct was obtained in which **1** alkylated either the 5'-AGC or 5'-GGC sequence.⁸ A 12-mer oligonucleotide [d(CGTAAGCTTACG)]₂ was prepared via phosphoramidite chemistry⁹ and then reacted with **1**^{10,11} to generate a 1:1 drug–DNA adduct. Nonexchangeable proton

* Author to whom correspondence should be addressed.

(1) Rinehart, K. L.; Holt, T. G.; Fregeau, N. L.; Stroh, J. G.; Keifer, P. A.; Sun, F.; Li, L. H.; Martin, D. G. *J. Org. Chem.* **1990**, *55*, 4512–4515.

(2) Sakai, R.; Jares-Erijman, E. A.; Manzanares, I.; Elipse, M. V. S.; Rinehart, K. L. *J. Am. Chem. Soc.* **1996**, *118*, 9017–9023.

(3) Sakai, R.; Rinehart, K. L.; Guan, Y.; Wang, A. H.-J. *Proc. Natl. Acad. Sci. U.S.A.* **1992**, *89*, 11456–11460.

(4) Guan, Y.; Sakai, R.; Rinehart, K. L.; Wang, A. H.-J. *J. Biomol. Struct. Dyn.* **1993**, *10*, 793–818.

(5) Corey, E. J.; Gin, D. Y.; Kania, R. S. *J. Am. Chem. Soc.* **1996**, *118*, 9202–9203.

(6) Pommier, Y.; Kohlhagen, G.; Bailly, C.; Waring, M.; Mazumder, A.; Kohn, K. W. *Biochemistry* **1996**, *35*, 13303–13309.

(7) Remers, W. A.; Iyengar, B. S. *Antitumor Antibiotics*. In *Cancer Chemotherapeutic Agents*; Foye, W. O., Ed.; American Chemical Society: Washington, DC, 1995; pp 577–679 and references therein.

(8) Unpublished results. The sites of drug modification were verified via 2D NOESY NMR.

(9) Gait, M. J., Ed.; *Oligonucleotide Synthesis—A Practical Approach*; IRL Press: Oxford, England, 1984.

(10) A gift from Dr. G. Faircloth, PharmaMar USA, Inc., Cambridge, MA.

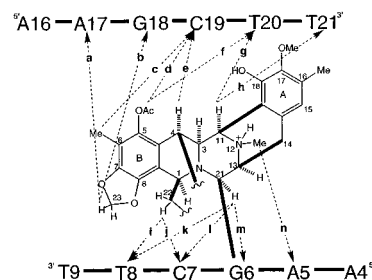


Figure 1. Schematic model of **1** bound to the 12-mer showing the critical NOE cross-peaks (arrows) that define the orientation of **1** in the minor groove of DNA (unit C of **1** has been omitted for clarity). Specific connectivities are (a) 17AH2 to H23A, (b) 18GH1' to H23A, (c) 19CH4'/H5'/H5'' to 6Me, (d) 19CH3'/H4' to OAc, (e) 19CH2'/H2'' to H4, (f) 20TH6 to OAc, (g) 20TH1'/H2''/H4' to H11, (h) 21TH5' to H11, (i) 8TH3' to H22B, (j) 7CH1' to H22A/22B, (k) 8TH1' to H21, (l) 7CH2'/2'' to H21, (m) 6GH1' to H21, and (n) 5AH2 to 12NMe.

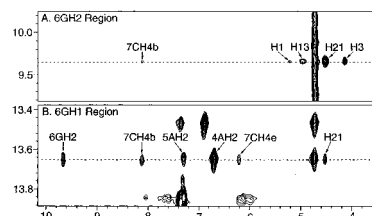


Figure 2. Connectivities of exchangeable protons in the **1**–12-mer adduct. (Panel A) Partial 2D water NOESY expansion contour plot of the 6GH2 cross-peaks into **1** and 7C protons. (Panel B) Partial 2D water NOESY expansion contour plot of the 6GH1 cross-peaks into 6GH2 and DNA. The broadness of some of the cross-peaks is due to overlap of 21TH3 to 4AH2 and 5AN2.

to proton connectivities in the adduct were determined using two-dimensional (2D) nuclear Overhauser effect spectroscopy (NOESY), correlation spectroscopy (COSY), and total correlation spectroscopy (TOCSY) experiments. Exchangeable protons were studied in an H₂O–D₂O (9:1) mixture via 2D NOESY experiments. The resulting spectra exhibited well-resolved cross-peaks for both **1** and the oligomer. Total assignment of the 12-mer oligonucleotide cross-peaks was achieved through established methods,¹² indicating that a single species was present in solution. Intramolecular NOEs for **1** were then used to assign the drug resonances; 47 residual cross-peaks were identified as **1** to DNA intermolecular contacts.

Analysis of **1** to 12-mer NOEs in the nonexchangeable NOESY spectrum yielded several critical connectivities that permitted the positioning of **1** in the minor groove (Figure 1). The NOEs between 5AH2 and 12NMe plus the 17AH2 to H23A contacts confirmed the presence of **1** in the minor groove, with the A unit to the 5' side of the alkylated 6G and the B unit to the 3' side. Units A and B are closely associated with the DNA strand opposite the 6GN2 alkylation, showing NOE connectivities between 18G, 19C, 20T, and 21T protons to the 6Me, 5OAc, H23, H4, and H11 protons. Upfield shifts of 19CH1', 19CH2', 19CH2'', and 18GH1' by 1.07, 0.55, 0.66, and 0.25 ppm, respectively, caused by the aromatic shielding cone over the 19C and 18G deoxyribose, provide additional evidence for the positioning of unit B. Interactions of **1** with the alkylated oligonucleotide strand are evidenced by NOEs between DNA and H21 and H22. The H21 proton shows NOEs into 6GH1', 7CH1', 8TH1', 7CH2'/H2'', 7CH6, and 8TH6. NOEs of H22A and H22B into 7CH1' and 8TH3' are also consistent with **1**

(11) The oligomer (14.2 mg, 1.9 μmol) was reacted with **1** (1.6 mg, 2.1 μmol, 1.1 equiv) in buffer (100 mM KCl, 50 mM potassium phosphate, pH 6.9) for 5 h at 25 °C. Unreacted **1** was removed by centrifugation.

(12) Hare, D. R.; Wemmer, D. E.; Chou, S. H.; Drobny, G.; Reid, B. R. *J. Mol. Biol.* **1983**, *171*, 319–336.

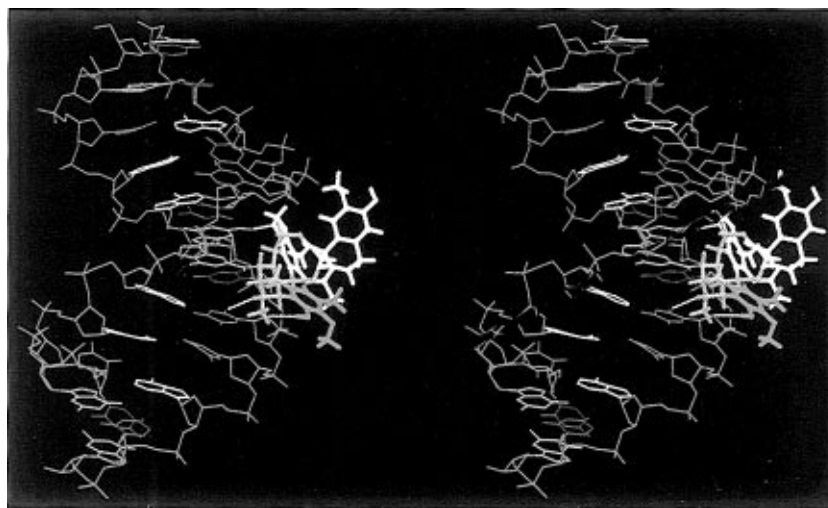


Figure 3. Stereoview of a molecular model of the **1**–oligonucleotide adduct derived from molecular dynamics analysis. The model depicts the orientations of unit A (green), unit B (yellow), and unit C (white) and their interactions with the adenine (gold), thymidine (red), guanosine (cyan), and cytosine (purple) residues in the minor groove of the 12-mer oligonucleotide. White dotted lines show proposed hydrogen bonding between units A and B and DNA, as described in the text.

being centered at 6G of the oligonucleotide. The surprising observation is the presence of only a single weak oligonucleotide–**1** NOE (8TH3'–7'OMe) involving unit C. The broadness observed in the intramolecular NOEs of unit C suggests that it is interconverting between conformations, i.e., not specifically associating with a site on the DNA. We believe that this is evidence that unit C is perpendicularly projected above the minor groove.

The exchangeable proton NOESY spectrum contained the predicted amino and imino interbase connectivities with an additional resonance at 9.57 ppm. We have observed that alkylation of GN2 by tomaymycin^{13a} and anthramycin^{13b} results in downfield shifts to 8.9 and 9.2 ppm, respectively, of the remaining N2 proton; therefore, the 9.57 resonance was assigned to 6GH2. The 6G2 proton showed an NOE to 19CH4 and 6GH1, and the latter showed the expected intermolecular NOEs to 7CH4b, 7CH4f, and 5AH2 (Figure 2). The through-space interactions between 6GH2 and **1** are associated with H1, H3, H13, and H21 that surround the carbinolamine in **1** (Figure 2). We believe that these data, combined with the nonexchangeable NOESY data, support the proposed alkylation of 6GN2 by **1** and the role of the carbinolamine in this reaction and define the position of **1** in the minor groove of the oligonucleotide.

We generated a model of **1** covalently bound to 6GN2 of the [d(CGTAAGCTTACG)]₂ oligonucleotide using solvated molecular dynamics¹⁴ (100 ps, AMBER version 4.1).¹⁵ The resulting model (Figure 3) is consistent with the NMR data and generally consistent with the existing theoretical models;⁴ however, there are differences between the model proposed here and that previously proposed.⁴ Our model positions unit B deeper into and closer to the wall of the nonalkylated strand than previously proposed⁴ while maintaining the hydrogen bond from the dioxymethylene oxygen to 18GH2 (Figure 3). Unit A is perpendicular to the helical axis and oriented to allow a hydrogen bond between 18OH and 21TO1' (Figure 3). The AT base pair to the 5' side of the alkylation site shifts the hydrogen bonds of the protonated 12NMe to 21TO2 and 21TO1'

as compared to the proposed amino/carbonyl pattern in the GC base pairs in the Wang et al. model.⁴ These ring orientations and hydrogen bonds are, in part, responsible for directing ring C centrally out of the minor groove, thereby restricting interactions with either side of the minor groove.

On the basis of our model and the reported sequence selectivity of **1**,⁶ we propose selectivity is partially dependent upon the number and spatial orientation of the hydrogen bond donor/acceptor sites. It is likely that a DNA hydrogen bond donor to the 3' side and hydrogen bond acceptors to the 5' side of the alkylation site are important. Et 743 seems to prefer a guanosine amino donor site on the nonalkylated strand and a 5'-side pyrimidine O2 as a hydrogen bond acceptor on the nonalkylated strand. Hydrogen bonding of 18OH to 20TO1', combined with the preference of **1** for donors/acceptors on the nonalkylated strand, seems to be responsible for tilting rings A and B toward the nonalkylated strand, thereby orienting ring C centrally out of the minor groove.

In conclusion, we believe that the model is important for the further development of the Ets as antitumor agents. Units A and B and the carbinolamine of **1** appear to be the critical structural features responsible for DNA recognition and bonding; therefore, this framework should be conserved in synthetic Et analogs. The paucity of C unit interactions with the DNA is significant in that (1) this functionality, at least in part, conveys antitumor selectivity and cytotoxic potency^{2,3} to the Ets and therefore is a site for chemical modifications and (2) in the total synthesis of **1**,⁵ this is the last functionality to be introduced, permitting analoging of the Ets from a common starting material. A key remaining question is whether the different C units that centrally protrude from the minor groove of various Et analogs can explain the unique activities of these different compounds based on interactions with DNA-recognizing or -processing enzymes.

Acknowledgment. We thank PharmaMar for a sample of Et 743. We are grateful to Dr. David Hoffman and Steve Sorey for NMR technical assistance. Research was supported by a grant from the National Institutes of Health (CA-49751). We also thank David Bishop for proofreading and editing the manuscript.

Supporting Information Available: NOESY spectra (2 pages). See any current masthead page for ordering and Internet access instructions.

JA9704500

(13) (a) Boyd, F. L.; Stewart, D.; Remers, W. A.; Barkley, M. D.; Hurley, L. H. *Biochemistry* **1990**, *29*, 2387–2403. (b) Unpublished results.

(14) Conditions for the dynamics analysis included periodic boundary conditions, temperature scaling using the Berendsen algorithm, and SHAKE constraints applied to bonds involving hydrogen.

(15) Pearlman, D. A.; Case, D. A.; Caldwell, J. C.; Wilson, R. S.; Cheatham, T. E., III; Ferguson, G. L.; Seibel, G. L.; Singh, U. C.; Weiner, D.; Kollman, P. A. *AMBER 4.1*; University of California: San Francisco, CA, 1995.